

THE STUDY OF EMA EFFECT ON MODAL IDENTIFICATION: A REVIEW

M.I. Ramli^{1,2}, M.Z. Nuawi^{1*}, S. Abdullah¹, M.R.M. Rasani¹, M.S. Salleh³, M.F. Basar⁴

¹Department of Mechanical and Materials Engineering,
Faculty of Engineering and Built Environment,
Universiti Kebangsaan Malaysia, 43600 Bangi, Selangor, Malaysia

²Department of Mechanical Engineering Technology,
Faculty of Engineering Technology,

³Department of Manufacturing Engineering Process,
Faculty of Manufacturing Engineering,

⁴Department of Electrical Engineering Technology,
Faculty of Engineering Technology,
Universiti Teknikal Malaysia Melaka,
Hang Tuah Jaya, 76100 Durian Tunggal, Melaka, Malaysia

ABSTRACT

Modal Analysis is a common practice to define parameters of structure under scientific view. The properties that come along need to be enlightened so that every circumstance appeared can be tackled in proper manner. Experimental Modal Analysis (EMA) is a well-known procedure for determining modal parameters. The EMA is regarded as an 'indoor tools' to examine modal parameters. Meanwhile, Operational Modal Analysis (OMA) on the other hand acts as an 'outdoor tools', or operated at site. OMA tests in most engineering applications are not comparable to typical EMA tests. During a typical OMA test, the structure has different boundary conditions than the typical free-free conditions of an EMA test. Therefore, it can be expected that OMA results in many (or even most) engineering applications will show higher damping values than a free-free EMA test. Here, the EMA analysis method will be discussed. Modal parameters consist of mode shape, natural frequency and damping ratio. The study focused on performing mass change strategy via mass normalization of the displacement and strain mode shape occurred in strain EMA. By applying EMA, the mass-normalized displacement and strain mode shapes of the structures can be obtained, through matching the shapes which were calculated by FEM. The results were verified via classic EMA measurement method. One of the benefit of applying mass change strategy is other than obtaining the modal parameter, the strain mode shape parameter also possible to be determined. From the analysis, one can understand that the EMA has its own significant role in detecting modal appeared by mean of vibration. Thus, EMA proven to be a useful method to gain relevant data relating with mechanical properties characteristics other than strain such like stress, impact, tensile, elongation etc.

KEYWORDS: EMA; OMA; Modal analysis; Mode shape; Natural frequency; Damping ratio.

* Corresponding author e-mail: mzn@ukm.edu.my

1.0 INTRODUCTION

Scientifically, Experimental Modal Analysis (EMA) is conducted to determine modal parameters that include examining outcome of natural frequency, mode shape and damping ratio. The knowledge of structural modal parameters is a must in order to define the natural frequencies, mode shapes and modal damping ratios (Wang & Cheng, 2011). EMA is a well-known procedure to determine modal analysis (Kranj et al., 2013). Meanwhile, Operational Modal Analysis (OMA) deals with the identification of modal parameters of a structure using output response of vibrated structures, without the knowledge of the forces causing the response and useful in determining large structures such as bridges, towers etc. (Modak, 2013). OMA is output-only modal method, where the excitation is performed with the ambient force, obtaining only relative values of the mode shapes (Zhang et al., 2004).

Previously, OMA, by which only the structural responses are used, has been widely applied and described in literature. OMA is attractive in many situations because it can be applied to structures in operation and does not require excitation, which is practical for many large structures (Rainieri & Fabbrocino, 2014 & Rainieri et al., 2016). Theoretically, modal parameters should be identically estimated via an OMA test and a classical EMA test (Ozbek & Rixen, 2016). However, it has still sometimes been reported that an EMA test is more reliable because of the available information and controlled environment (Orlowitz & Brandt, 2015).

Dynamic characteristics such as mode shapes and modal frequencies of the unstrengthened and the strengthened structure were individually determined through experimental modal analysis (EMA) and numerical analysis (Cakir et al., 2016).

EMA is considered reliable because it is based on input-output system identification, which allows validation e.g. of the estimated frequency response functions (FRFs) by coherence functions. However, the strength of EMA is also limiting its applicability as it requires that all inputs (excitation forces) are measured, which is practically unfeasible for many structures (Orlowitz & Brandt, 2017). The main issue here is whether EMA method could deliver an outstanding outcome to apprehend the result in tackling environment issue related to sound.

2.0 MODAL ANALYSIS

Generally, Modal Analysis is conducted to acquire two basic modal parameters which are natural frequencies and mode shapes. Modal Analysis solve for natural tendencies of the structure in the form of motions and frequencies. Vibration occurs in all scenarios of design to some extent. Even when designing steel in a building, a Modal Analysis is helpful to understand what happen in the event of an earthquake or even equipment that running in a building that might cause a sense of vibration. Two classification of Modal Analysis are Operational Modal Analysis (OMA) and Experimental Modal Analysis (EMA) (Xu & Zhu, 2013). Modal Analysis is derived originally from Equation of Motion which stated that every motion occurs is incorporated with vibration alongside it (Inman, 2013) as shown in Figure 1.

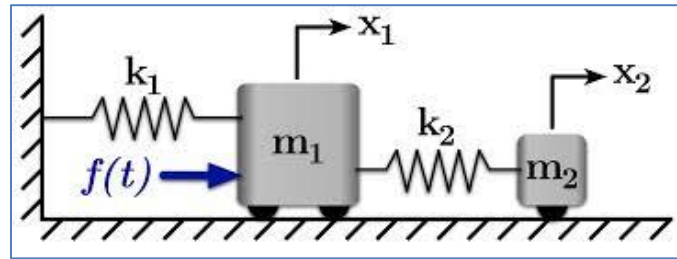


Figure 1. Spring equation of motion (Inman, 2013)

$$m_1\ddot{x}_1 + (k_1 + k_2)x_1 - k_2x_2 = 0 \quad (1)$$

$$m_2\ddot{x}_2 - k_2x_1 + k_2x_2 = 0 \quad (2)$$

or in matrix,

$$\begin{bmatrix} m_1 & 0 \\ 0 & m_2 \end{bmatrix} \begin{Bmatrix} \ddot{x}_1 \\ \ddot{x}_2 \end{Bmatrix} + \begin{bmatrix} k_1 + k_2 & -k_2 \\ -k_2 & k_2 \end{bmatrix} \begin{Bmatrix} x_1 \\ x_2 \end{Bmatrix} = \begin{bmatrix} 0 \\ 0 \end{bmatrix} \quad (3)$$

or

$$m\ddot{x} + kx = 0 \quad (4)$$

The natural frequency is derived as follows:

$$\omega_n = \sqrt{\frac{k}{m}} \quad (5)$$

(ω_n = natural frequency, k = spring stiffness, m = mass, x = displacement from static equilibrium position)

Here, natural frequency appears which shall bear with mode shapes once the vibration takes place.

Mode shapes on the other hand is obtained through displacement (eigenvectors) that is subjected to scaling procedure which referred as mass-normalization with respect to the orthogonality properties of the mass-normalized modal matrix (Maia & Silva, 1997).

3.0 REVIEW OF RELEVANT WORK

3.1 Experimental Modal Analysis (EMA)

Prediction of the responses of the structures against dynamic effects such as earthquakes is very important in terms of seismic safety (Yang et al., 2013). Therefore, dynamic parameters such as frequency, mode shape and damping ratio must be determined. In the studies about determination of dynamic parameters, experimental tests are great importance. In order to determine the dynamic parameters various procedures can be applied. Especially, the dynamic parameters such as mode shapes and modal frequencies can be determined by using natural or forced vibrations (Tran et al., 2016). While the natural vibrations are traffic or wind effects, the forced vibrations are vibrodyne or hammer effects (Codispoti et al., 2015; Tomazevic et al., 2015).

EMA, is also known as frequency response function test, is one of the most important of the experimental tests and it is based on measurement of the vibration response of the

impact applied to the structure (Cakir, 2014). EMA adapts the principle of the response measurement of the load applied to the structural system (Cakir & Uysal, 2015). The modal parameters of the structural system are determined through the structural response by the load applied. Therefore, EMA has been frequently preferred for the determination of modal parameters (Crossley et al., 2013; Acar et al., 2013). In the EMA test, the research area was isolated and all devices that can vibrate were closed against undesirable external influence in order to obtain the most accurate results (Pela et al., 2013).

EMA is a technique used to determine the natural frequencies and modes of vibration of a structure. Similar to operational modal analysis, the process consists of measuring the acceleration of a structure at numerous points (Wittich & Hutchinson, 2016). In contrast to operational modal analysis, EMA provides a known input to excite the vibration of the structure and increases the signal-to-noise ratio (Parisi & Augenti, 2013; Wittich et al., 2014). While this input can be applied as harmonic input from a portable shaker or an impulse from an impact hammer, portable shakers may inadvertently excite other objects in the vicinity of the intended test specimen, in addition to the target. As a result, EMA with an impact hammer is the ideal choice for determining the natural frequencies of the as-built statue-pedestal-restraint systems (Aktas & Turer, 2015; Harvey et al., 2014; Wittich & Hutchinson, 2015). It should be noted that this technique not only requires multiple sensors to be in direct contact with the structure, but also requires contact at the point of impact of the hammer (Wittich & Hutchinson, 2015).

A new approach to the mass normalization in a strain EMA, without using a motion sensor is reviewed. The approach is based on the latest introduced mass-changed structural modification method which is used for the mass normalization of an OMA (Kranj et al., 2013). When the displacement mode shapes of a dynamical system are not scaled following to the orthogonal properties of the mass-normalized modal matrix, they cannot be used for the calculation of mass and stiffness matrices (Bernasconi & Ewins, 1989). Usually, mass-normalized displacement mode shapes of a real structure are determined using an EMA (Heylen et al., 2007). The other modal parameters are also determined using the same EMA. Here, the less frequently used strain EMA also can be applied to determine modal parameters by using strain sensor to measure the response (Bernasconi & Ewins, 1989). In addition to modal parameters, the strain mode shapes parameter is also possible to be obtained (Bernasconi & Ewins, 1989).

3.1.1 Theoretical Background

a) The strain response of a dynamical system

The strain response of a dynamical system was derived from the motion response. The motion steady-state response $X_{(\omega)}$ of the hysteretically proportionally damped dynamical system can be written as (Maia & Silva, 1997):

$$\mathbf{X}_{\omega} = \mathbf{\Phi} [\omega_r^2 (1 + i\eta_r) - \omega^2]^{-1} \mathbf{\Phi}^T \mathbf{F}(\omega) = \mathbf{H}(\omega) \mathbf{F}(\omega) \quad (6)$$

Where $\mathbf{\Phi}$ is the modal matrix (matrix of mass-normalized displacement mode shapes), ω_r are the natural frequencies, η_r are the damping loss factors, $\mathbf{F}(\omega)$ is the vector of the excitation force, $\mathbf{H}(\omega)$ is the receptance matrix and $[\cdot]$ stands for a diagonal matrix.

b) Strain EMA

The strain EMA can be used for determining the dynamical properties of a real structure, similar to the classic EMA (Bernasconi & Ewins, 1989). During the strain modal testing, a structure is excited with a known force at the structure point k and the response is determined with a strain measurement at the point j . In order to obtain the information about the displacement and the strain mode shapes, at least one row and one column of the strain FRF matrix need to be experimentally determined (Yam et al., 1996).

The identification of natural frequencies and the damping is performed in a similar way as in the classic EMA (Yam et al., 1996). Hence, the results of an indirect modal identification method (Maia & Silva, 1997) are the natural frequencies, the damping (Slavic et al., 2003), the strain modal constants and their phases for all the measures strain FRF. The strain modal constants that are identified from the j th row and k th column of the strain FRF matrix are denoted as ${}_r\mathbf{A}_j^\varepsilon = \phi_{jr}^\varepsilon \Phi_r$ and ${}_r\mathbf{A}_k^\varepsilon = \Phi_r^\varepsilon \phi_{kr}$, respectively. ${}_r\mathbf{A}_j^\varepsilon$ and ${}_r\mathbf{A}_k^\varepsilon$ contain the information about Φ_r and Φ_r^ε respectively.

c) Mass normalization using the mass-change strategy in the OMA

In this research, the mass normalization in the strain EMA is performed with the mass-change strategy that is normally used for the mass normalization of the displacement mode shapes in the OMA (Parloo et al., 2002; Aenlle et al., 2010). The process of the mass-change strategy for the OMA is shown in Figure 2.

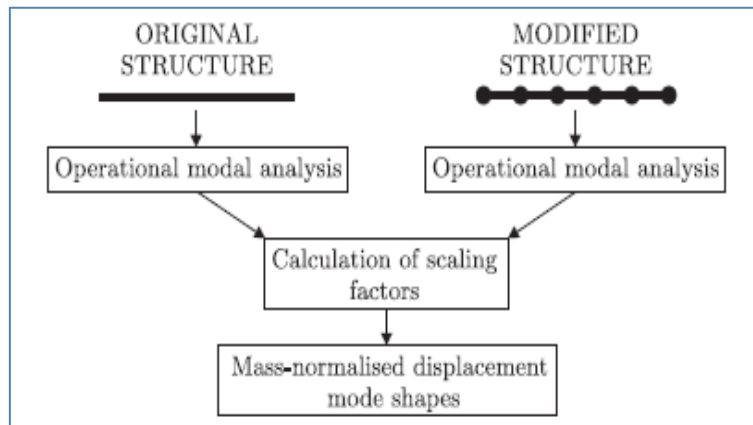


Figure 2. The process of the mass-change strategy in the OMA (Vandiver et al., 1982)

Given Φ_r = mass-normalized displacement mode shapes (Ewins & Gleeson, 1982) and Ψ_r = unnormalized displacement mode shapes, with scaling factors α_r which are used for the calculation of Φ_r , the relation between Ψ_r and Φ_r is express as (Parloo et al., 2002; Aenlle et al., 2005)

$$\Phi_r = \alpha_r \Psi_r \tag{7}$$

(Parloo et al., 2002) developed an approach that uses a first-order approximation for the sensitivity of the natural frequencies of lightly damped structures as follows,

$$\alpha_r = \frac{2(\omega_r - \omega_{m,r})}{\omega_r \Psi_r^T \Delta \mathbf{m} \Psi_r} \tag{8}$$

Where $\Delta\mathbf{m}$ is the mass-change matrix. The application of this expression requires small frequencies shifts and thus small structure modifications. Suggestion was made that mass changes around 5%. From Equation of Motion (Brincker & Andersen, 2003),

$$\alpha_r = \sqrt{\frac{(\omega_r^2 - \omega_{m,r}^2)}{\omega_{m,r}^2 \Psi_r^T \Delta\mathbf{m} \Psi_r}} \quad (9)$$

Below is the expression that considers the displacement mode shapes before and after the modification (Aenlle et al., 2005).

$$\alpha_r = \sqrt{\frac{(\omega_r^2 - \omega_{m,r}^2)}{\omega_{m,r}^2 \Psi_r^T \Delta\mathbf{m} \Psi_{m,r}}} \quad (10)$$

Where α_r is the scaling factors, ω_r is natural frequencies, $\omega_{m,r}$ is modified structure natural frequencies, Ψ_r is unnormalized displacement mode shapes, $\Delta\mathbf{m}$ is mass change matrix and $\Psi_{m,r}$ is unnormalized displacement mode shapes of the modified structure.

d) Mass normalization with a mass-change strategy for the strain EMA

The mass normalization in the strain EMA will be conducted by modifying the mass-change strategy for OMA. The procedure for the mass-change strategy for the strain EMA (Figure 3) is similar with OMA.

Initially, the strain EMA is performed on an original structure to determine the information about displacement mode shapes, the strain mode shapes, the natural frequencies and the damping of the structure. The unnormalized displacement and strain mode shapes are identified from the j th row and k th column of the strain FRF matrix, respectively. Then, the structure modification is performed in the same way as in in the mass-change strategy for the OMA. Next, the strain EMA is performed on a modified structure to determine the information about the displacement mode shapes and the natural frequencies of the modified structure.

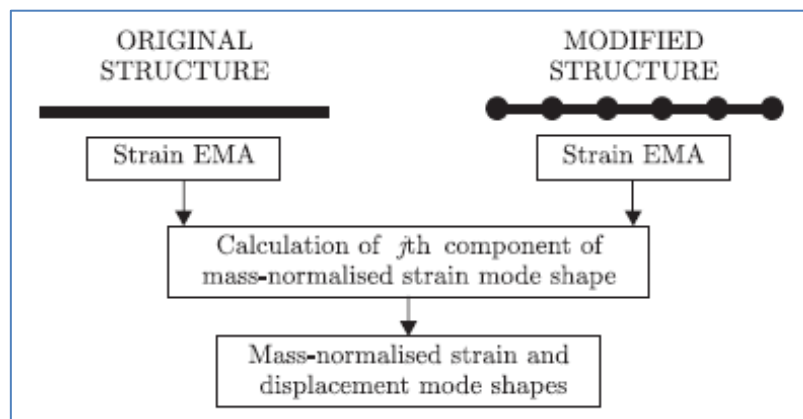


Figure 3. The process of the mass-change strategy in the strain EMA (Kranj et al., 2013)

Finally, the calculation of the scaling factors for the mass normalization in the strain EMA shall be obtained. Replacing Ψ_r in Eq. (7) with the identified displacement mode shape (unnormalized) ${}_r\mathbf{A}_j^\varepsilon$ produced the relation as shown below.

$$\alpha_r = (\phi_{jr}^\varepsilon)^{-1} \quad (11)$$

This prove that the scaling factor for the r th mode is the j th inverse component of the mass-normalized strain mode shape Φ_r^ε . The expressions for the calculation of the scaling factors that use the mass-change strategy are modified to calculate the ϕ_{jr}^ε . Thus, Eqs. (8) – (10) can be rewritten as:

$$MC\phi_{jr}^\varepsilon = \sqrt{\frac{\omega_r({}_rA_j^\varepsilon)^T \Delta m({}_rA_j^\varepsilon)}{2(\omega_r - \omega_{m,r})}} \quad (12)$$

$$MC\phi_{jr}^\varepsilon = \sqrt{\frac{\omega_{m,r}^2({}_rA_j^\varepsilon)^T \Delta m({}_rA_j^\varepsilon)}{(\omega_r^2 - \omega_{m,r}^2)}} \quad (13)$$

$$MC\phi_{jr}^\varepsilon = \sqrt{\frac{\omega_{m,r}^2({}_rA_j^\varepsilon)^T \Delta m({}_rA_{m,j}^\varepsilon)}{(\omega_r^2 - \omega_{m,r}^2)}} \quad (14)$$

Where $MC\phi_{jr}^\varepsilon$ is the j th component of Φ_r^ε that is estimated with the mass-change strategy for the strain EMA. $MC\phi_{jr}^\varepsilon$ is used for a determination of the mass-normalized displacement and strain mode shapes using the following equations:

$$\Phi_r = \pm \frac{{}_rA_j^\varepsilon}{MC\phi_{jr}^\varepsilon} \quad (15)$$

$$\Phi_r^\varepsilon = \pm \frac{{}_rA_k^\varepsilon MC\phi_{jr}^\varepsilon}{{}_rA_{jk}^\varepsilon} \quad (16)$$

3.1.2 Objective and Scope of Work

The study was to perform the mass normalization of the displacement and strain mode shapes in strain EMA (Kranj et al., 2013). The work is focused by using recently introduced mass-change strategy for OMA (Parloo et al., 2002; Brincker & Andersen, 2003; Aenlle et al., 2005) that was modified in such a way that it was applicable to strain EMA. Additionally, the study used experimental test of a free-free supported beam and plate for validation (Kranj et al., 2013).

3.1.3 Experimental Works

Experimental modal analysis is a non-destructive testing, based on vibration response of the structures. The technique widely used in modal analysis, is based on impact hammer excitation (Prasad & Seshu, 2008). It is well known that (mechanical) structures can resonate, i.e. small forces can result in important deformation, and possibly, damage can be induced in the structure. The majority of structures can be made to resonate, that is to vibrate with excessive oscillatory motion (Walunj et al., 2015; Allan & Thomas, 2010). Predominately, EMA is used to explain a dynamics problem, vibration or acoustic, which is not obvious from intuition, analytical models or previous similar experience. Experimental modal analysis methods involve the theoretical relationship between measured quantities and the classic vibration theory. All modern methods trace from the matrix differential equations yield a final mathematical form in terms of measured data.

This measured data can be raw input and output data in the time or frequency domains or some form of processed data such as impulse response or frequency response functions (Anuar, et al., 2012). Mathematically, the frequency response function (FRF) is defined as the Fourier transform of the output divided by the Fourier transform of the input. The measurements taken during a modal test are FRF measurements. The parameter estimation routines are, in general, curve fits in the Laplace domain and result in the transfer functions (Zhang, 2004). Theoretically, when a structure is excited by external excitation matrix, the output matrix (such as displacement, velocity and acceleration) can be tested in an experiment (Siringoringo, et al., 2008; Lee, et al., 2008).

To validate the proposed method, experimental tests on a beam and a plate structure were performed.

a) Experimental tests on a beam structure

By referring to Figure 4 and Figure 5, the experimental apparatus consists of steel, 1m long free-free supported beam with a rectangular 0.01 x 0.03m cross-section were prepared. The free-free boundary conditions were achieved by suspending the structure from thin ropes.

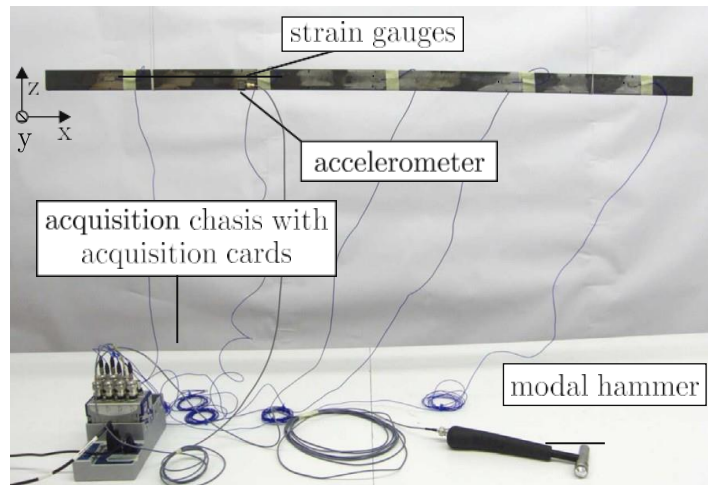


Figure 4. The strain modal testing on the free-free supported beam (Kranj et al., 2013)

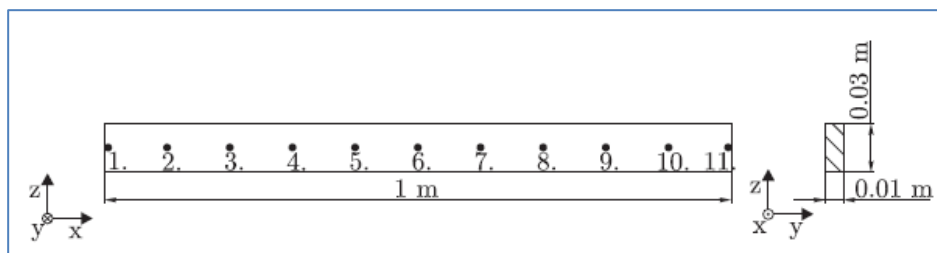


Figure. 5. The tested beam (Kranj et al., 2013)

Only the bending modes in the plane xy were considered, that results in displacements in the y -direction and normal strains in the x -direction (Hutton, 2003). The experiment was performed as follows. First, the strain EMA was performed and then the mass-normalization procedure with the mass-change strategy for the strain EMA followed. The results were compared to the results of the finite element method (FEM) and then used for a reconstruction of the measured accelerances (Kranj et al., 2013).

During the strain modal testing the response was measured in the x -axis (Figure 5) with calibrated strain gauges (PCB 740B02), while the structure was excited with a modal hammer (B&K Type 8206-002) in the y -axis. First, the responses were measured at structure point 4 (Figure 5), while the structure was excited at the points 1-11 to determine the 4th row of the 11 x 11 sized strain FRF matrix. Then the responses were measured at the points 2, 4, 6, 8, 10 while the structure was excited at the point 4 to determine the 4th column of the strain FRF matrix. With five strain gauges that were attached to the structure, only the 2nd, 4th, 6th, 8th and 10th elements of the 4th column were measured (Kranj et al., 2013).

The tested structures are lightly damped; therefore, the modal parameter identification was performed with the Ewins-Gleeson identification method (Ewins & Gleeson, 1982), which was developed for such structures, assuming the hysteretic damping model.

The displacement and strain mode shapes were mass normalized using the proposed mass-change strategy for the strain EMA. The strain EMA for the original structure follows the structure modification by attaching magnets to the structure points 1-11 (Figure 5). Each of the magnets weighted 11.6g and the total mass of the magnets was approximately 5.4% of the original structure weight. After the structure modification the strain EMA was performed for the modified structure once again. The natural frequencies of the modified beam were decreased by the added mass (Kranj et al., 2013).

b) Experimental tests on a plate structure

The second experimental was performed on a steel, 0.4 x 0.32 x 0.003m sized, free-free supported plate (Figure 6). Consider the first five modes vibrate out of plane xy and result in the normal and shear strains (stresses) (Leissa, 1969). The application of the proposed approach was shown by determining of the mass-normalized displacement mode shapes and the normal components of the mass-normalized strain mode shapes in the x -direction and the y -direction.

The strain modal testing was performed with the same equipment as in the case of the beam. To gather the information about the displacement mode shapes the plate was excited with the modal hammer at the points 1-30 (Figure 6) and the response was measured at the point 31. The information about the strain mode shapes was obtained by exciting the structure at the point 26 and measuring the normal x -components of the strains at the points 6, 11, 16, 21, 31 and the normal y -components at the points 2-4. The modal identification was performed in a similar way as in the case of the beam. That is followed the mass normalization by the proposed approach. In order to ensure that the mass change will not affect the displacement mode shapes, the magnets were attached as follows. At the points (7-9, 12-14, 17-19, 22-24), (2-4, 6, 10, 11, 15, 16, 20, 21, 25, 27-29) and (1, 5, 26, 30) the 11.6g, 5.1g and 3.6g magnets were attached to the structure respectively. The total mass of the magnets was approximately 6.6% of the original structure's weight (Kranj et al., 2013).

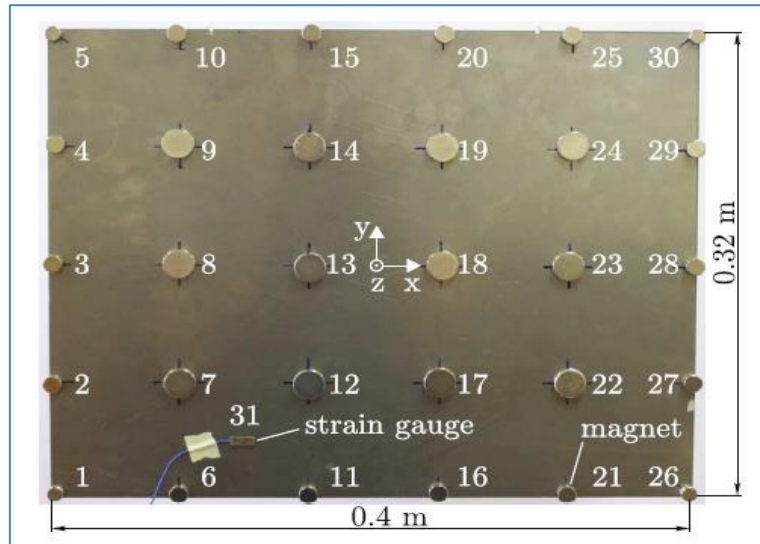


Figure 6. The experimental testing on the free-free supported plate (Kranj et al., 2013)

3.1.4 Result and Discussion

a) Beam Structure

Strain EMA

Figure 7 shows the difference between the displacement mode shapes identified using strain EMA and the calculated strain mode shape by FEM (mass-normalized). Figure 7 (a, c, e, g, i) and (b, d, f, h, j) shows the first five displacement and strain mode shapes respectively. The result shows that the experimentally determined mode shapes are not in agreement with the calculated ones. The discrepancies are the result of incorrect scaling. Therefore, the experimentally determined mode shapes match the calculated ones only in the mode shape nodes (Figure 7 (c) and (d), the structure point 6 at the 2nd displacement and strain mode shapes) (Kranj et al., 2013).

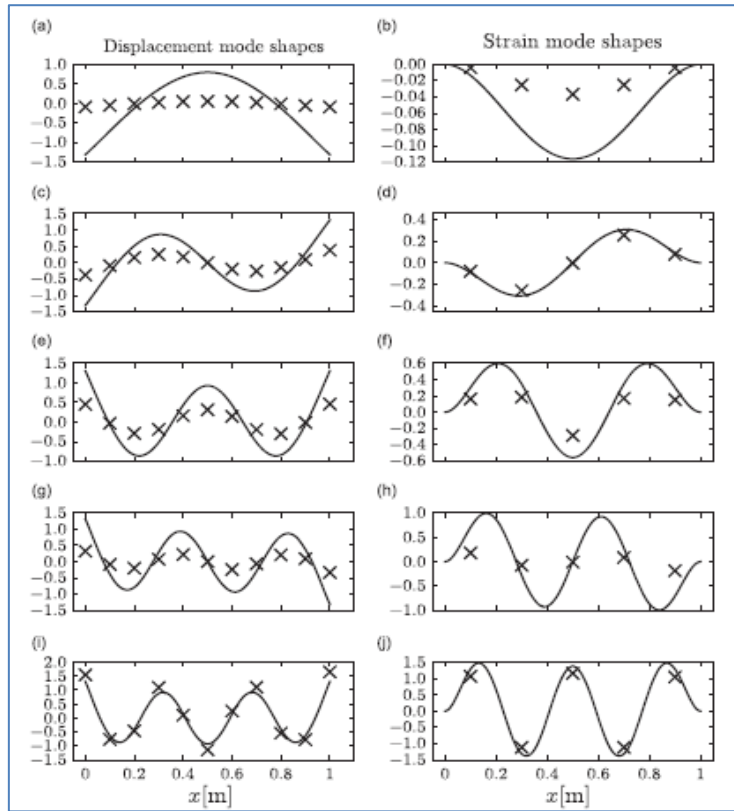


Figure 7. The first five displacement (a, c, e, g, i) and strain (b, d, f, h, j) mode shapes; determined with the strain EMA (unnormalized) “x”, calculated using FEM (mass normalized) “-“ (Kranj et al., 2013)

Mass normalization with the mass-change strategy for the strain EMA

Table 1 shows the change evident, with f_r and $f_{m,r}$ stand for natural frequencies of the original and modified structures respectively, and δ_r is the relative change between the natural frequencies of the original and modified structures. The displacement mode shapes that are determined using the strain EMA are scaled by the j th component of the strain mode shape ϕ_{jr}^ε . To calculate ϕ_{jr}^ε one of Eqs. (12) – (14) can be used. In order to choose the appropriate approach a comparison of the displacement mode shapes before and after the structure modification was performed using the modal assurance criterion (MAC) (Allemang, 1982). Figure 8 show that the displacement mode shapes were not significantly changed by the structure modification, thus Eq. (13) was used.

Table 1. Natural frequencies of the original and the modified beams (Kranj et al., 2013)

r	f_r [Hz]	$f_{m,r}$ [Hz]	δ_r [%]
1	52.85	51.05	-3.41
2	145.45	140.45	-3.44
3	285.00	274.70	-3.61
4	471.10	454.20	-3.59
5	701.25	675.05	-3.74

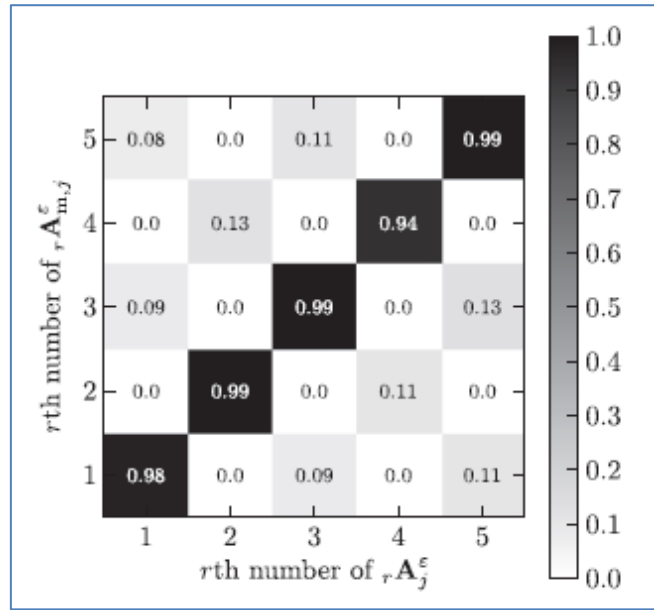


Figure 8. The correlation between the displacement mode shapes of the original and the modified beams (Kranj et al., 2013)

$MC\phi_{jr}^{\epsilon}$ were then calculated for all modes and used to determine the mass-normalized displacement and the strain mode shapes Φ_r and Φ_r^{ϵ} with Eqs. (15) and (16). The Φ_r and Φ_r^{ϵ} that were determined with the proposed approach are plotted together with the calculated ones using FEM. Figure 9 shows the first five displacement and strain mode shapes respectively. From the figure we can see that the experimental results match the calculated ones as it is (Kranj et al., 2013).

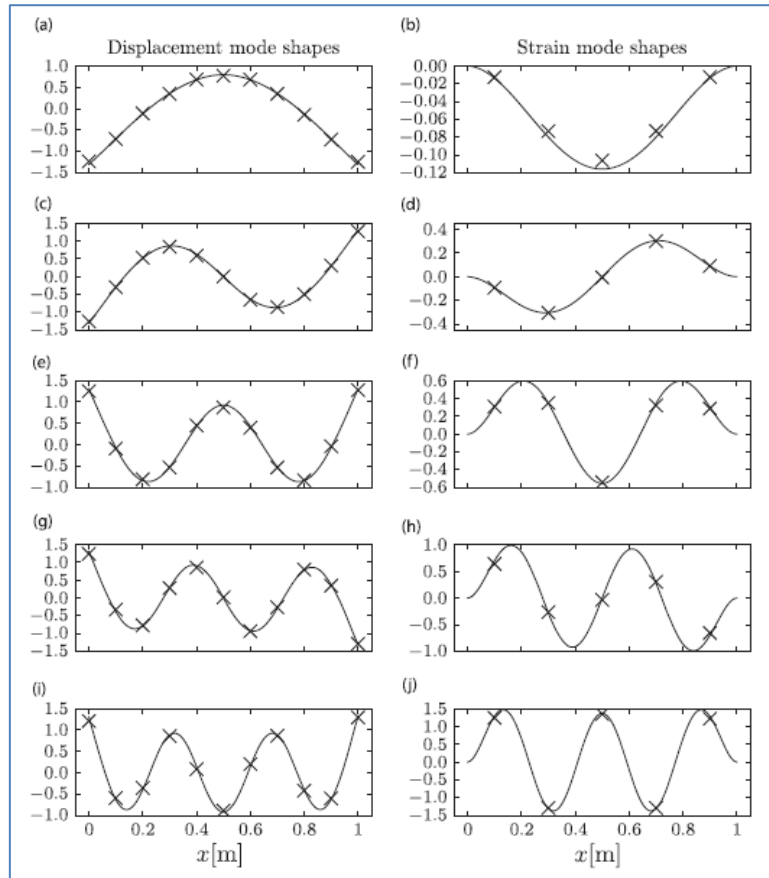


Figure 9. The first five mass-normalized displacement (a, c, e, g, i) and strain (b, d, f, h, j) mode shapes; determined with the proposed approach “x”, calculated using FEM “-“ (Kranj et al., 2013)

b) Plate Structure

The natural frequencies before and after the modification are shown in Table 2 in which f_r stands for natural frequencies before modification and $f_{m,r}$ for natural frequencies after modification. The relative frequency shifts are denoted as δ_r . The displacement mode shapes were not affected by the modification. By using MAC comparison of ${}_r\mathbf{A}_j^\varepsilon$ and ${}_r\mathbf{A}_{m,j}^\varepsilon$, it proved that the modification did not affect the displacement mode shapes.

Table 2. Natural frequencies of the original and the modified plates (Kranj et al., 2013)

r	f_r [Hz]	f_{mr} [Hz]	δ_r [%]
1	80.10	77.40	-3.40
2	98.20	94.60	-3.70
3	167.10	160.10	-4.20
4	191.80	184.80	-3.60
5	224.20	215.10	-4.10

Eq. (13) is used for the calculation of ${}_M\mathbf{C}\Phi_{31r}^\varepsilon$, that were used after for mass-normalization. The testing results consist of the components of Φr at points (1-30) and the components $\Phi_r^{\varepsilon_{xx}}$ and $\Phi_r^{\varepsilon_{yy}}$ at points (6, 11, 16, 21, 31) and (2-4) respectively.

The experimental results were compared to the FEM results. The comparison at the experimentally determined Φ_r versus the calculated ones. The relative comparison was performed by MAC analysis. Figure 10 (a, c, e, g, i) shows Φ_r for the structure points 1-30. The detailed plots are shown in Figure 10 (b, d, f, h, j), where only the components of Φ_r at the location $y = -0.08\text{m}$ are plotted. Then, the experimentally determined components of Φ_r^ε were compared to the calculated ones by FEM in Figure 11.

Figure 11 (a, c, e, g, i) shows the $\Phi_r^{\varepsilon xx}$ at the location $y = -0.16\text{m}$. Figure 11 (b, d, f, h, j) shows $\Phi_r^{\varepsilon yy}$ at the location $x = -0.2\text{m}$. From the result, the experimentally determined components of Φ_r and Φ_r^ε are in good agreement with the calculated ones.

Nevertheless, there are some discrepancies occurred such like errors due to measuring errors, local stiffness changes due to strain gauges that are attached to the relatively thin sheet metal and the deviations of the strain-gauge attachment regarding the position and the angle (Kranj et al., 2013).

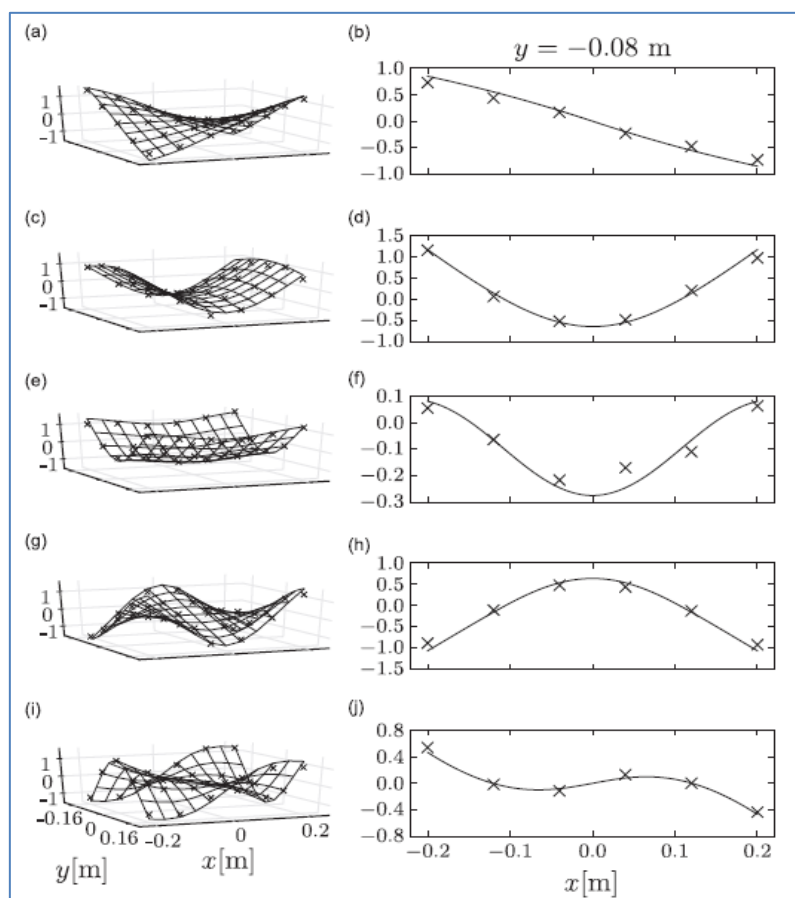


Figure 10. The first five mass-normalized displacement mode shapes ((a, c, e, g, i) – all the measuring points, (b, d, f, h, j) – points at $y = -0.08\text{m}$); calculated (-) and experimentally determined (x) (Kranj et al., 2013)

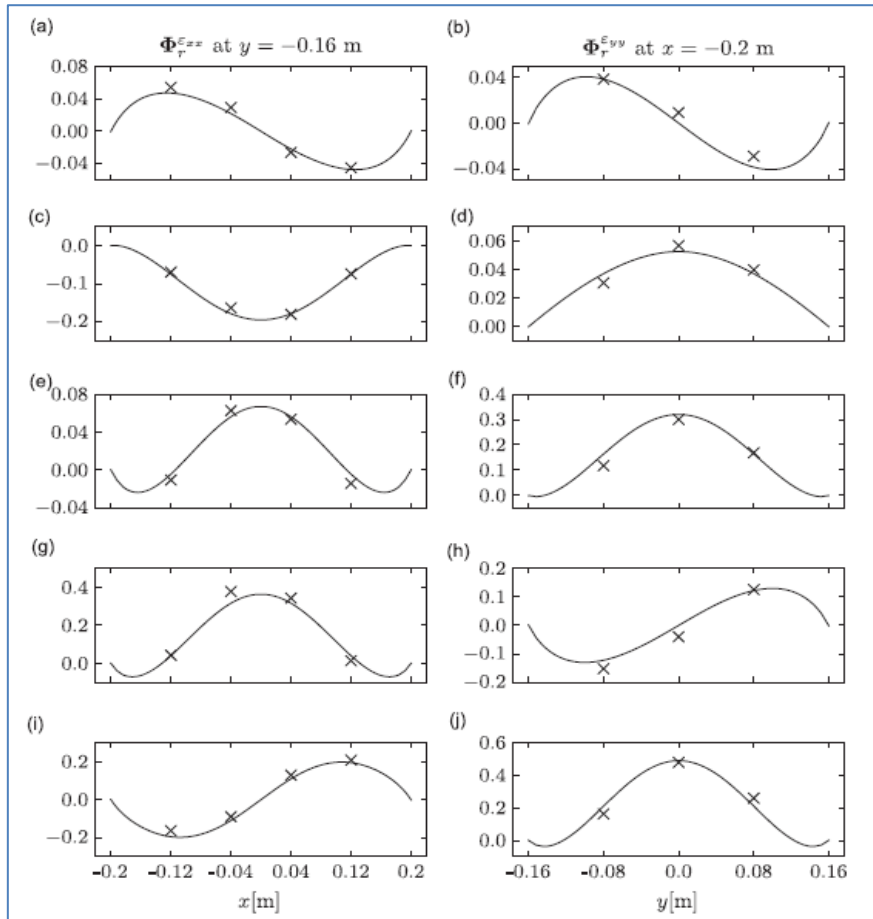


Figure 11. Components of the first five mass-normalized strain mode shapes ((a, c, e, g, i)- $\Phi_r^{\epsilon_{xx}}$, (b, d, f, h, j)- $\Phi_r^{\epsilon_{yy}}$; calculated (-) and experimentally determined (x) (Kranj et al., 2013)

4.0 CONCLUSION

The characteristics of EMA have been reviewed. It was clear that by applying EMA, the mass-normalized displacement and strain mode shapes of the structures can be obtained, by matching the shapes which were calculated by FEM. The results showed very good agreement and were verified via classic EMA measurement method and can be proposed for the reconstruction of the measured direct accelerances. One of the benefit of applying mass change strategy is other than obtaining the modal parameter, the strain mode shape parameter also possible to be determined. The result has its own validity with the proposed approach.

From the analysis, it was clear that the EMA have its own significant role in detecting modal appeared by mean of vibration. Thus, EMA proven to be a useful method to gain relevant data relating with mechanical properties characteristics other than strain such like stress, impact, tensile, elongation etc. The idea of applying mechanical properties characteristics such as strain in this study has contributes in widening the understanding of getting relevant information on structure just by relying on the EMA method.

ACKNOWLEDGEMENTS

The authors would like to thank Universiti Teknikal Malaysia Melaka (UTeM) and the Ministry of Higher Education Malaysia (MOHE) for financial support of this study. Much appreciation also goes to Universiti Kebangsaan Malaysia (UKM) for the financial support under research grant ERGS/1/2013/TK01/UKM/02/2. Also thank you to Assoc. Professor Dr. Mohd. Zaki Nuawi for the assistance and advices.

REFERENCES

- Acar, V., Akbulut, H., Sarikanat, M., Seydibeyoglu, M.O., Seki, Y. & Erden, S. (2013). Enhancement of interface mechanics of carbon fiber reinforced prepreg composites with carbon nanostructures. *Journal of Machine Technology*. 10 (3): 43-51.
- Aenlle, M.L., Brincker, R. & Canteli, A.F. (2005). Some methods to determine scaled mode shapes in natural input modal analysis. In *Proceedings of the 23rd. International Modal Analysis Conference (IMAC-XXIII)*. Orlando, Florida, USA.
- Aenlle, M.L., Fernandez, P. & Brincker, R. (2010). A. Fernandez-Canteli, Erratum to scaling-factor estimation using an optimized mass-changed strategy. *Mechanical Systems and Signal Processing*. 24 (8): 3061-3074.
- Aktas, Y.D. & Turer, A. (2015). Seismic evaluation and strengthening of nemrut monuments. *Journal of Cultural Heritage*. 16: 381-385.
- Allan, G.P. & Thomas, L.P.H. (2010). *Shock and Vibration Handbook*. The McGraw-Hill Co., Inc., 6th. Edition.
- Allemang, R.J. (1982). A correlation coefficient for modal vector analysis. In *Proceedings of the 1st International Modal Analysis Conference (IMAC-1)*. Orlando, Florida, USA. pp. 110-116.
- Anuar, M.A., Mat Isa, A.A. & Ummi, Z.A.R. (2012). Modal characteristics study of cem-1 single -layer printed circuit board using experimental modal analysis. *Procedia Engineering*. 41: 1360-1366.
- Bernasconi, O. & Ewins, D.J. (1989). Application of strain modal testing to real structures. In *Proceedings of the 7th. International Modal Analysis Conference (IMAC-VII)*. pp. 1453-1464.
- Bernasconi, O. & Ewins, D.J. (1989). Modal strain/stress fields. *The International Journal of Analytical and Experimental Modal Analysis*. 4 (2): 68-76.
- Brincker, R. & Andersen, P. (2003). A way of getting scaled mode shapes in output only modal analysis. In *Proceedings of the 21st. International Modal Analysis Conference (IMAC) XXI*. Orlando, USA. pp. 141-145.

- Cakir, F. (2014). Strengthening of masonry arches with nano particles reinforced composite materials (PhD Thesis), *Graduate School of Natural and Applied Sciences*, Ataturk University, Erzurum, Turkey.
- Cakir, F. & Uysal, H. (2015). Experimental modal analysis of brick masonry arches strengthened prepreg composites. *Journal of Cultural Heritage*. 16: 284-292.
- Cakir, F., Uysal, H. & Acar, V. (2016) Experimental modal analysis of masonry arches strengthened with graphene nanoplatelets reinforced prepreg composites. *Measurement*. 90: 233-241.
- Codispoti, R., Oliviera, D.V., Olivito, R.S., Laurengo, P.B. & Fanguero, R. (2015) Mechanical performance of natural fiber reinforced composites for the strengthening of masonry. *Composites Part B*. 77: 74-83.
- Crossley, R.J., Schubel, P.J. & De Focatiis. (2013). Time-temperature equivalence in the tack and dynamic stiffness of polymer prepreg and its application to automated composites manufacturing. *Composites Part A*. 52: 126-133.
- Ewins, D. & Gleeson, P. (1982). A method for modal identification of lightly damped structures. *Journal of Sound and Vibration*. 84 (1): 57-79.
- Harvey, P.S., Zehil, G.P. & Gavin, H.P. (2014). Experimental validation of a simplified model for rolling isolation systems. *Earthquake Engineering Structure Dynamic*. 43: 1067-1088.
- Heylen, W., Lammers, S. & Sas, P. (2007). *Modal Analysis Theory and Testing*. Katholieke Universiteit Leuven, Haverlee.
- Hutton, D. (2003). *Fundamentals of Finite Element Analysis*. *Engineering Series*. McGraw-Hill Professional Publishing.
- Inman, D.J. (2013). *Engineering Vibration*, 4th. Edition. Prentice Hall, USA.
- Kranj, T., Slavic, J. & Boltezar, M. (2013). The mass normalization of the displacement and strain mode shapes in a strain experimental modal analysis using the mass-change strategy. *Journal of Sound and Vibration*, 332: 6968-6981.
- Lee, Y.C., Wang, B.T., Lai, Y.S., Yeh, C.L. & Chen, R.S. (2008). Finite element model verification for packaged printed circuit board by experimental modal analysis. *Microelectronics Reliability*. 48(11-12): 1837-1846.
- Leissa, A. (1969). *Vibration of Plates*. *NASA SP, Scientific and Technical Information Division, National Aeronautics and Space Administration*.
- Maia, N. & Silva, J. (1997). *Theoretical and Experimental Modal Analysis, Mechanical Engineering Research Studies: Engineering Dynamic Series*. John Wiley & Sons Ltd.

- Modak, S.V. (2013). Separation of structural modes and harmonic frequencies in operational modal analysis using random decrement. *Mechanical System and Signal Processing*. 41: 366-379.
- Orlowitz, E. & Brandt, A. (2015). Producing simulated time data for operational modal analysis. In *Proceedings of International Modal Analysis XXXIII*, Orlando, Florida, USA.
- Orlowitz, E. & Brandt, A. (2017). Comparison of experimental and operational modal analysis on a laboratory test plate. *Measurement*. 102: 121-130.
- Ozbek, M. & Rixen, D.J. (2016) A new analysis methodology for estimating the eigenfrequencies of systems with high modal damping. *Journal of Sound and Vibration*. 361: 290-306.
- Parisi, F. & Augenti, N. (2013). Earthquake damages to cultural heritage constructions and simplified assessment of artworks. *Engineering Failure Analysis*. 34: 735-760.
- Parloo, E., Verboven, P., Guillaume, P. & Van Overmeire, M. (2002). Sensitivity-based operational mode shape normalization. *Mechanical Systems and Signal Processing*. 16: 757-767.
- Pela, L., Aprile, A. & Benedetti, A. (2013). Comparison of seismic assessment procedures for masonry arch bridges. *Construction Building Materials*. 38: 381-394.
- Prasad, D.R. & Seshu, D.R. (2008). A study on dynamic characteristics of structural materials using modal analysis. *Asian Journal of Civil Engineering (Building and Housing)*. 9(2): 141-152.
- Rainieri, C. & Fabbrocino, G. (2014). Operational modal analysis of civil engineering structures, *Springer*.
- Rainieri, C., Dey, A., Fabbrocino, G. & Magistrisa, F.S. (2016). Interpretation of the experimentally measured dynamic response of an embedded retaining wall by finite element models, *Measurement*.
- Siringoringo, D.M. & Fujino, Y. (2008). System identification of suspension bridge from ambient vibration response. *Engineering Structures*. 30: 462-477.
- Slavic, J., Simonovski, I. & Boltezar, M. (2003). Damping identification using a continuous wavelet transform: Application to real data. *Journal of Sound and Vibration*. 262 (2): 291-307.
- Tran, T.D., Schlegel, H. & Neugebauer, R. (2016). Application of modal analysis for commissioning of drives on machine tools. *Procedia CIRP*. 40: 115-120.
- Tomazevic, M., Gams, M. & Berset, T. (2015). Strengthening of stone masonry walls with composite reinforced coatings. *Build. Earthquake Engineering*. 13: 2003-2027.

- Vandiver, J.K., Dunwoody, A.B., Campbell, R.B. & Cook, M.F. (1982). A mathematical basis for the random decrement vibration signature analysis technique. *Journal of Mechanical Design*. 104: 307-313.
- Walunj, P.S., Chougule, V.N. & Mitra, A.C. (2015). Investigation on modal parameters of rectangular cantilever beam using experimental modal analysis. *Materials Today: 4th. International Conference on Materials Processing and Characterization*. 2: 2121-2130.
- Wang, B.T. & Cheng, D.K. (2011). Modal analysis by free vibration response only for discrete and continuous systems. *Journal of Sound and Vibration*. 330: 3913-3929.
- Wittich, C.E., Hutchinson, T.C., Lo, E., Meyer, D. & Kuester, F. (2014). The South Napa Earthquake of August 24, 2014: Drone-based Aerial and Ground-based Li-DAR Imaging Survey. *Structural Systems Research Project Report SSRP-2014/09*, University of California, San Diego, USA.
- Wittich, C.E. & Hutchinson, T.C. (2015). Shake table tests of stiff, unattached, asymmetric structures. *Earthquake Engineering Structure Dynamic*. 44: 2425-2443.
- Wittich, C.E. & Hutchinson, T.C. (2015). Shake Table Tests of Stiff, Unattached, Asymmetric Structures-Phase 2: Pedestal-Mounted. *Structural Systems Research Project Report SSRP-2015/05*, University of California, San Diego, USA.
- Wittich, C.E. & Hutchinson, T.C. (2016). Experimental modal analysis and seismic mitigation of statue-pedestal systems. *Journal of Cultural Heritage*. 20: 641-648.
- Xu, Y. F. & Zhu, W.D. (2013). Operational modal analysis of a rectangular plate using non-contact excitation and measurement. *Journal of Sound and Vibration*. 332: 4927-4939.
- Yang, X., Wang, Z., Xu, M., Zhao, R. & Liu, X. (2013). Dramatic mechanical and thermal increments of thermoplastic composites by multi-scale synergetic reinforcement: Carbon Fiber and Graphene Nanoplatelet. *Material Design*. 44: 74-80.
- Yam, L., Leung, T., Li, Di & Xue, K. (1996). Theoretical and experimental study of modal strain analysis. *Journal of Sound and Vibration*. 191 (2): 251-260.
- Zhang, L., Brincker, R. & Andersen, P. (2004). An overview of operational modal analysis: Major development and issues. In *Proceedings of the 22nd. International Modal Analysis Conference (JMAC-XXII)* pp. 179-190.
- Zhang, L. (2004). An overview of major developments and issues in modal identification. In *Proceedings of the 22nd. International Modal Analysis Conference (IMAC-XXII)*. Detroit, Michigan, USA.